Supporting Information for

Redox-Active Modification of Dawson-Type Copper Molybdate Cluster for Advanced Supercapacitor Applications

Ankita Pardiwala[1], Ravi Rajan Pandey[2], Anshu Andola[2], Rakesh K. Pandey[2]*, and Ritambhara Jangir[1]*

[1]Sardar Vallabhbhai National Institute of Technology, Ichchanath, Surat-395 007, Gujarat, India.

[2]Department of Chemistry, Mahatma Gandhi Central University, East-Champaran, Motihari 845401, Bihar, India

*Corresponding Author: ritambhara.jangir@chem.svnit.ac.in, rakeshpandey@mgcub.ac.in

Table of Contents:

Schemes and Figures

Figure S13. Working prototype of the symmetric supercapacitor device.

Figure S14. (a) EIS before cycling test (b) EIS after 10000 cycle test.

Table S1. Crystallographic Data and Refinement Parameters of Complex **1.**

Table S2. Electrochemical Performance Comparison of State-of-the-Art POM Electrodes for Supercapacitors.

Table S3. Fractional Atomic Coordinates ($\times 10^4$) and Equivalent Isotropic Displacement Parameters ($Å^2 \times 10^3$) for **1**. U_{eq} is defined as 1/3 of of the trace of the orthogonalised U_{IJ} tensor.

Table S4. Anisotropic Displacement Parameters ($Å^2 \times 10^3$) for **1**. The Anisotropic displacement factor exponent takes the form: $-2\pi^2[h^2a^{*2}U_{11}+2hka^*b^*U_{12}+\ldots]$.

Table S5. Bond Lengths for **1**.

Table S6. Bond Angles for **1**.

Table S7. Hydrogen Atom Coordinates ($Å \times 10^4$) and Isotropic Displacement Parameters ($Å^2 \times 10^3$) for **1.**

Table S8. Atomic Occupancy for **1.**

Table S9. Solvent masks information for **1**.

S1. Materials

Molybdate trioxide (MoO_3), copper(II)nitrate dihydrate ($Cu(NO_3)_2 \cdot 2H_2O$) and dimethyl formamide (DMF), were purchased from Sigma Aldrich, DMF were received from Spectrochem. All the reagents and solvents were of analytical grade, hence were used without any further purification.

S2. Characterization

Fourier transform infrared (FT-IR) spectroscopy: FT-IR spectra were recorded using a SHIMADZU IR Affinity-1 Instrument; 45 scans were collected at a resolution of 4 cm^{-1}.

Thermo-gravimetric analysis: Thermogravimetric Differential thermal analyzer (TGA DTA) TA Module Q 600 system was used for thermogravimetric analysis.

Thermogravimetric analyses (TGAs) with purge and protection functions were performed at a nitrogen (N2) gas flow rate of 20 ml/min. At a rate of 10 K/min, the samples were heated from room temperature (RT) to 800°C.

Powder X-ray diffraction: Powder XRDs were carried out using a X-Ray Diffractometer (Panalytical X Pert Pro) instrument. The data analysis was performed using the Reflex module of the Materials Studio V6.0.

Field Emission-Scanning Electron Microscopy (FE-SEM): FE-SEM was performed using a Nova Nano FE-SEM 450 (FEI) scanning electron microscope. Pt sputtering was applied to the samples for 100s before observation

X-ray photoelectron spectroscopy (XPS): XPS was performed using a the Thermo Scientific Nexsa G2 X-Ray Photoelectron Spectrometer (XPS) System offers fully automated, high-throughput surface analysis, delivering the data to advance research and development or to solve production problems.

S3. Experimental Section

2.2 Synthesis of Copper incorporated well Dawson POMos *i.e.* $[(DMA)_3]^{3+}[H_9Cu_2Mo_{18}O_{62}]^{3-}$ (1).

A mixture of MoO_3 (6.89 g, 47.98 mmol), Cu $(NO_3)_2 \cdot 2H_2O$ (1.00 g, 4.47 mmol) along with DMF (35 ml) and H_2O (15 ml) was kept under stirring until a clear solution was obtained. The solution was stirred at 100 ℃ for 4 hours. A clear blue solution was kept undisturbed for crystallization. Blue needle crystals of appeared after about one weeks of slow evaporation at room temperature. Yields: 79%. IR (KBr, cm^{-1}): 3425 (br), 3101 (w), 1970 (s), 1635 (s), 1424 (m), 1103 (m), 910 (s), 833 (s), 845 (m), 648 (w).

2. X-ray single-crystal data collection and refinement

A suitable single crystal of **1** with dimensions of 0.23 × 0.21 × 0.19 mm^3, was picked using an optical microscope and sealed to a glass tube. Crystallographic data were collected using a 'Bruker APEX-II CCD' diffractometer with Mo Kα radiation at 295.0 K. Using Olex2[1], The structure was solved with the ShelXT[2] structure solution program using intrinsic phasing and refined with the ShelXL[3] refinement package using least squares minimization. The anisotropic displacement parameters were refined for all non-hydrogen atoms. Hydrogen

atoms on ligands are added to the riding model. Crystal data and structural refinements are summarized in table S2. Selected bond lengths (Å) and angles (°) of **1** are listed in table S3-S8. Crystallographic data for **1** are deposited in the Cambridge Crystallographic Data Center with CCDC 2479938.

S4. Electrochemical study

Three Electrode System: To stitch with working electrode support, 8 mg of synthesized of **1**, 1 mg of poly(vinylidene difluoride) (PVDF) binder, and 1 mg of super-p were mixed in 1 mL of N-methyl-2-pyrrolidone (NMP) solvent for a three-electrode setup. The slurry is applied onto a 0.5 mm graphite sheet (0.5 cm × 0.5 cm) as a working electrode for a three-electrode setup. The working electrode was dried overnight (~12-16 hours) at 80 °C in hot air oven then left at room temperature (~25°C) for an additional overnight period for remove residual solvent.

Symmetrical supercapacitor: Following the three-electrode system, the slurry was made with **1**, PVDF, and super-p in 8:1:1 to fabricate negative and positive electrodes. The slurry is applied onto a 0.5 mm graphite sheet (0.5 cm × 0.5 cm) as both negative and positive electrodes. The working electrode was dried overnight (~12-16 hours) at 80 °C in hot air oven then left at room temperature (~25°C) for an additional overnight period for remove residual solvent.

Supercapacitor Fabrication: A sandwich-type device with fabricated electrodes (positive and negative) separated by an NKK membrane, and Ni wire was used for the connection.

Instruments. Electrochemical analysis is performed by a potentiostat (Squidstat Plus by Admiral Instruments USA). During the experiments, Prior to data acquisition, 50 consecutive cyclic voltammetry (CV) cycles were performed at a scan rate of 100 mV/s in both the three-electrode and symmetric cell configurations to stabilize the electrode–electrolyte interface and ensure reproducible electrochemical behavior. All CV and GCD experiments performed 3 cycles and then use 3rd cycle response for data analysis. For Cs retention analysis, the 1st cycle response of CV was ignored [4].

Calculations:

For both three electrode and two electrode setups (solid state device, SC), the specific capacitance (C_s) calculated from the CV curves according to the following formula [5, 6]:

$$C_s(F/g) = \frac{\int_{E_i}^{E_f} i(E)d(E)}{\eta(E_f - E_i)m}$$

Where, E_i and E_f are initial potential (V) and final potential (V) respectively. $\int_{E_i}^{E_f} i(E)d(E)$ is total charge (area) under the CV curve. η and m are scan rate (V/s) and mass of electrode (g) respectively.

The specific capacitance (C_s) calculated from the discharging curves of GCD For both three electrode SCs according to the following formula[5]:

$$C_s\,(F/g) = \frac{i\Delta t}{(E_f - E_i)m}$$

Where, E_i, E_f, Δt and m are initial potential (V), final potential respectively (V), discharging time (s) and m is the mass (g).

For SCs (two electrode setup) energy density (E_d) calculated from the GCD according to the following formula [7, 8]:

$$E_d(Wh/g) = \frac{Cs \times (dV)^2}{7200}$$

Where, dV is the potential window derived from the GCD curves excluding the iR drop.

The power density (P_d) for SCs calculated from the GCD according to the following formula [7, 8]:

$$P_d\left(\frac{Wh}{g}\right) = \frac{E_d}{\Delta t} \times 3600$$

And *Rser* for SCs calculated from the GCD according to the following equation:

$$Rser = \frac{V_{drop}}{2i}$$

Where, i is current.

S5. Characterization of (**1**):

Figure S1. (a) Crystals of compounds **1**.

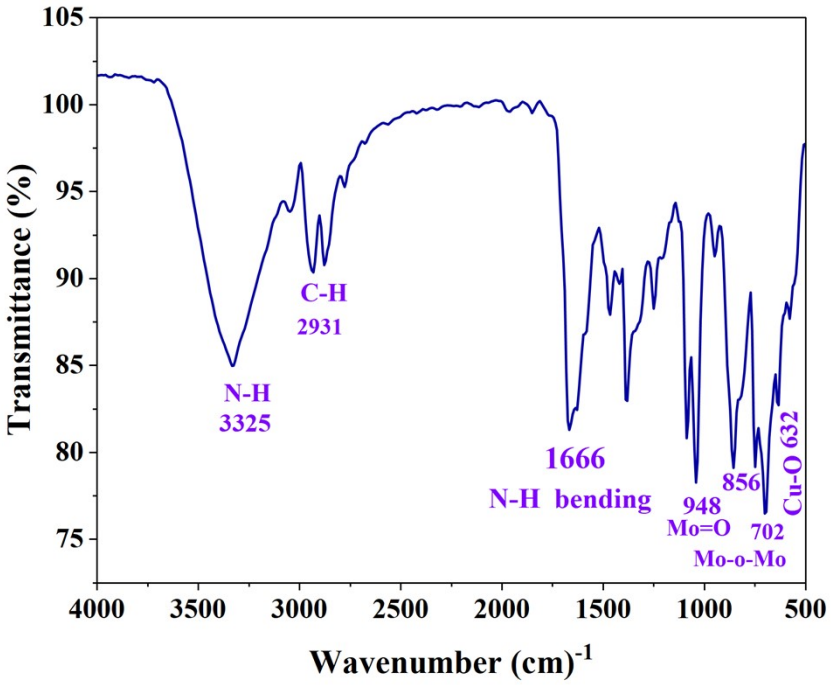

Figure S2. Fourier transform-infra-red (FT-IR) spectrum of **1**.

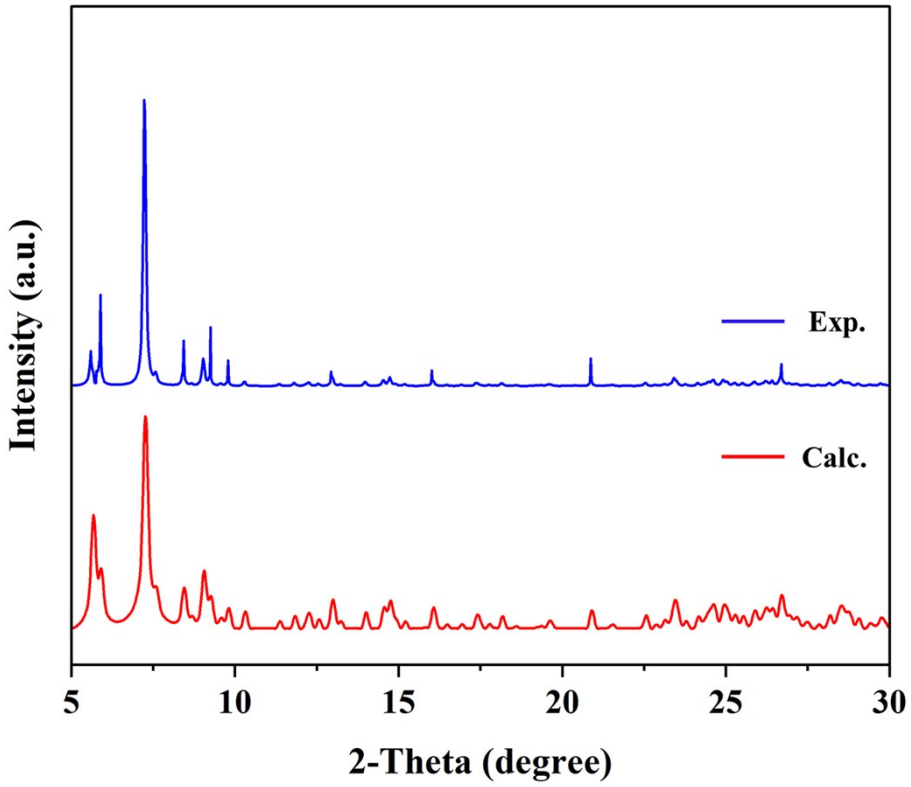

Figure S3. PXRD patterns (Exp. *vs* Calc.) of **1**.

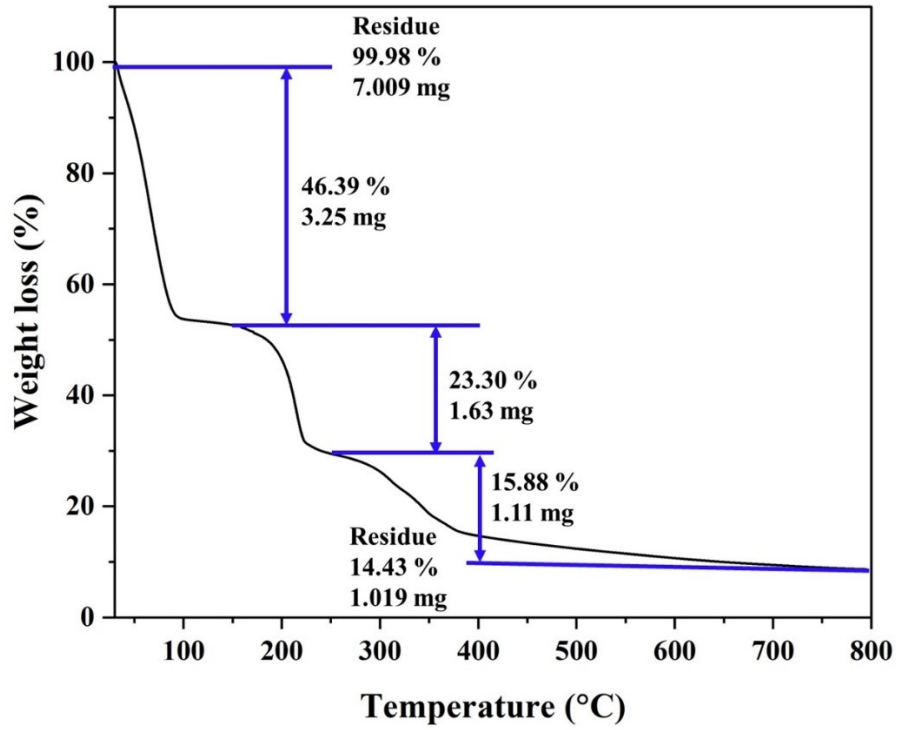

Figure S4. TGA curve of **1** (10°C/min, N_2 atm).

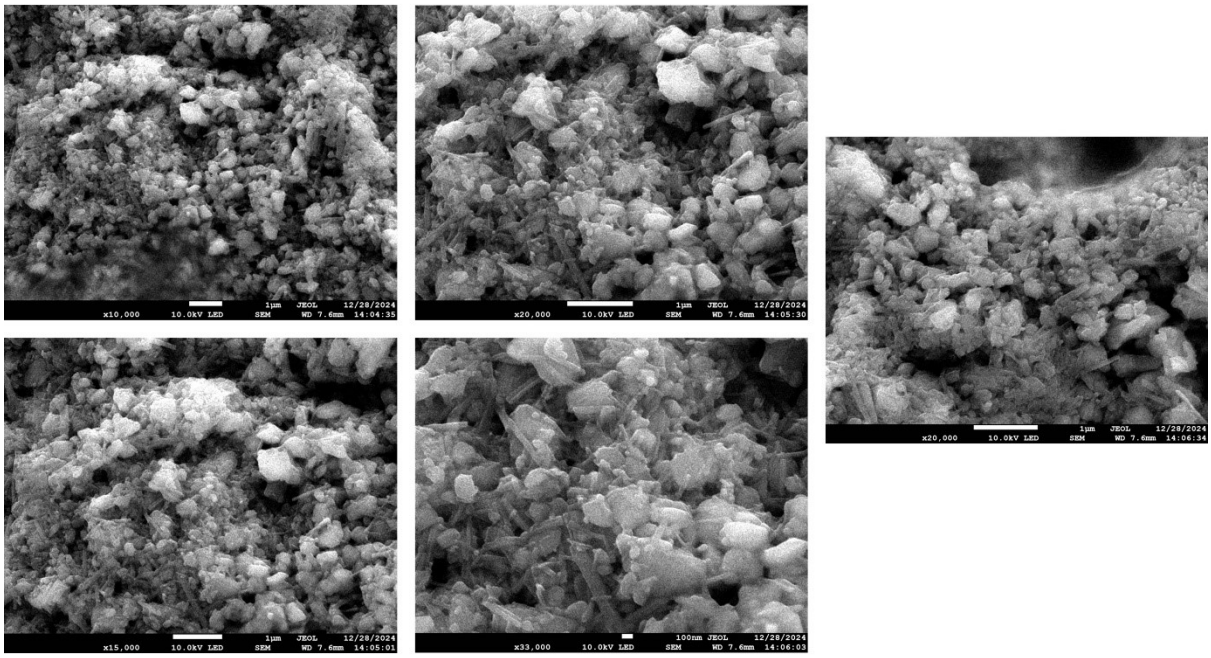

Figure S5. FE-SEM images of **1** at different resolutions.

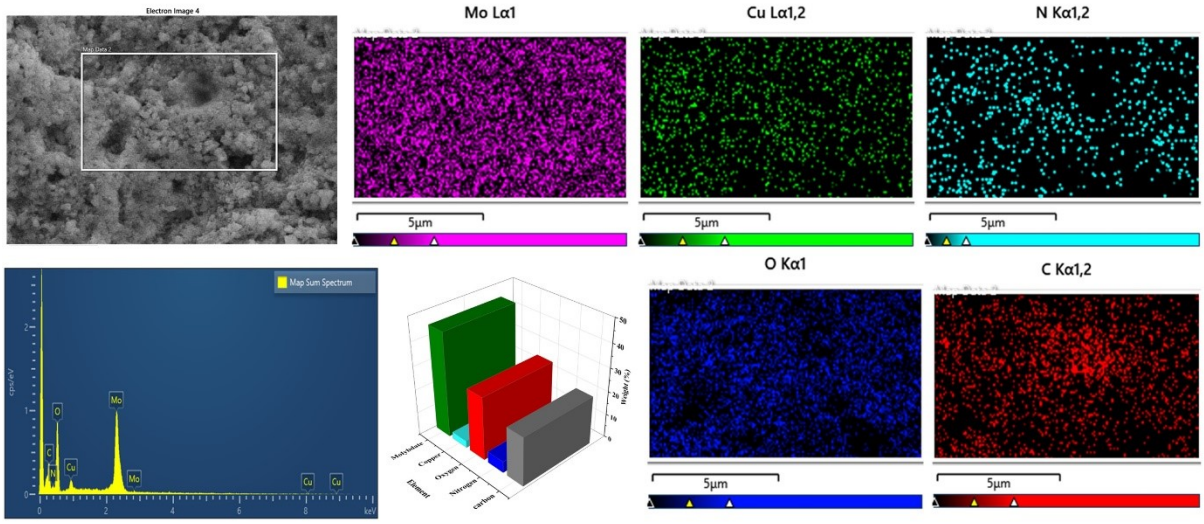

Figure S6. Energy dispersive X-ray spectroscopy (EDS) mapping of **1** in terms of composition elements C, N, O and Mo.

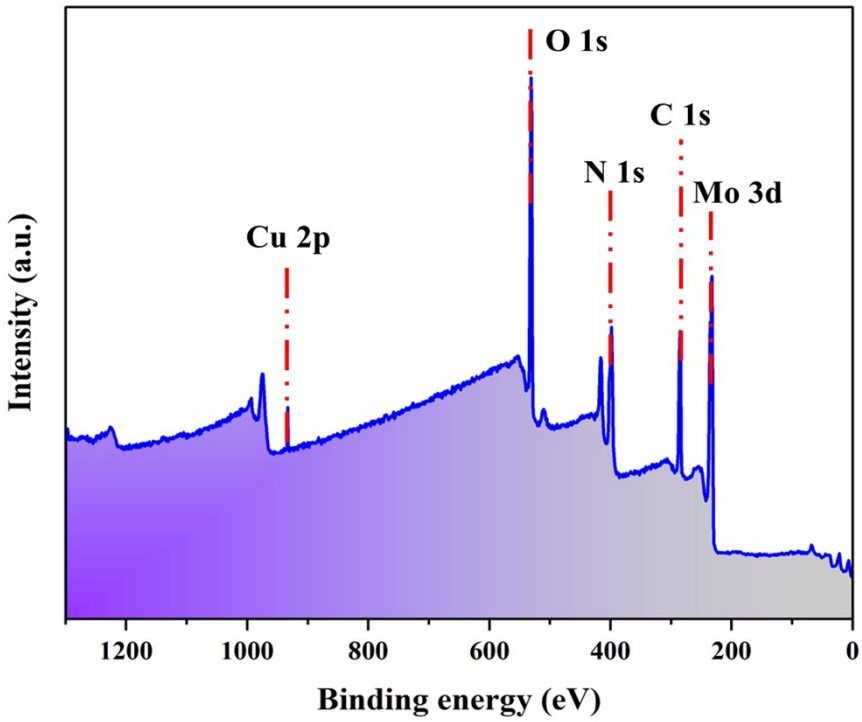

Figure S7. X-ray photoelectron spectroscopy (XPS) of **1**.

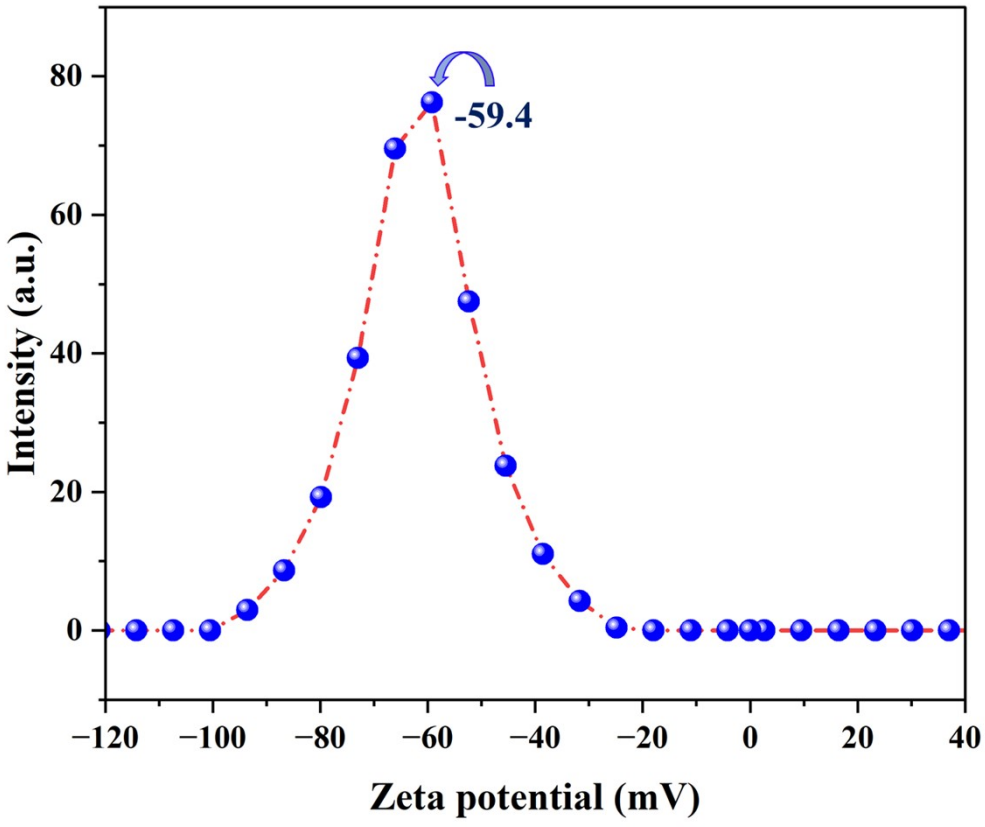

Figure S8. Zeta potential of **1**.

S6. Molecular structure of 1:

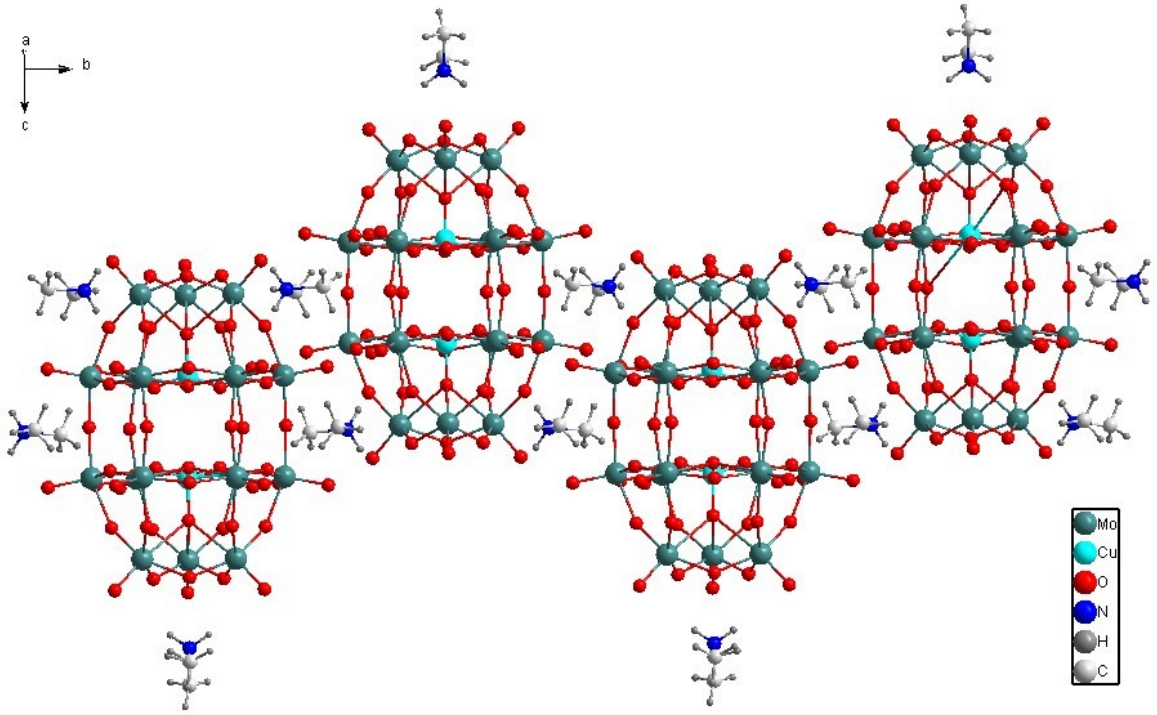

Figure S9. The structural motifs in a ball-and-stick representation, illustrating the 1D supramolecular architecture of **1**.

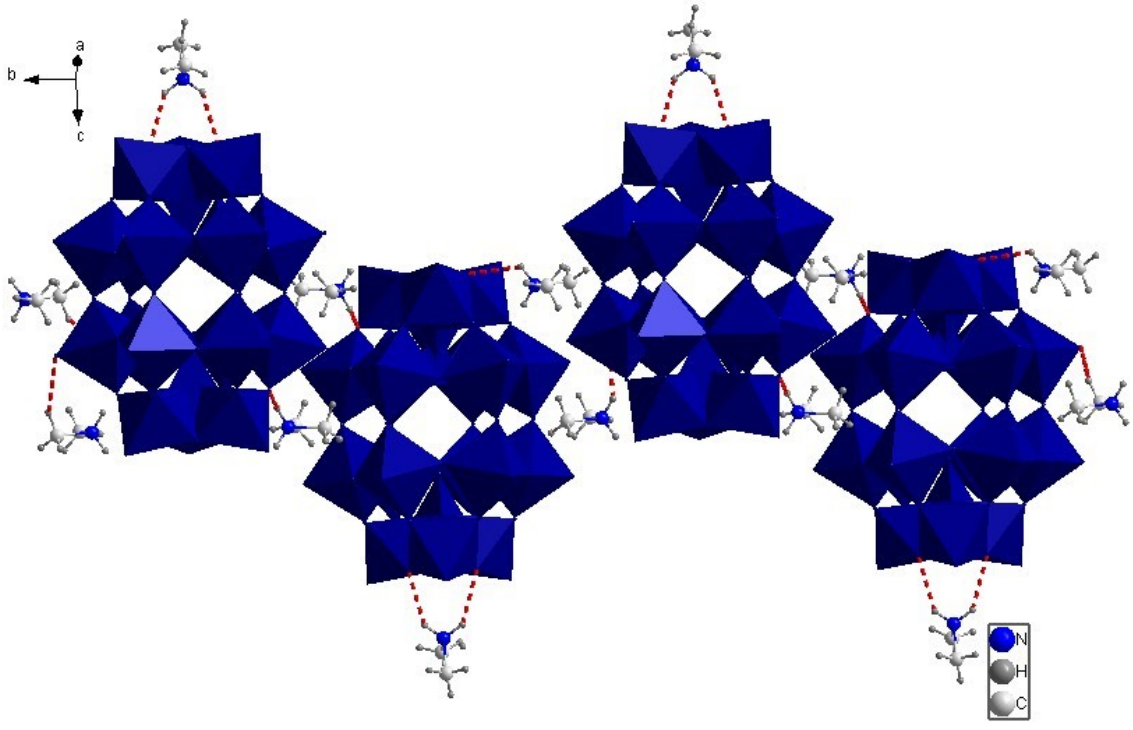

Figure S10: Polyhedral representation showing the $[H_9Cu_2Mo_{18}O_{62}]^{3-}$ anions as dark blue polyhedra, highlighting the extended hydrogen-bonded network (red dashed lines) mediated by organic cation.

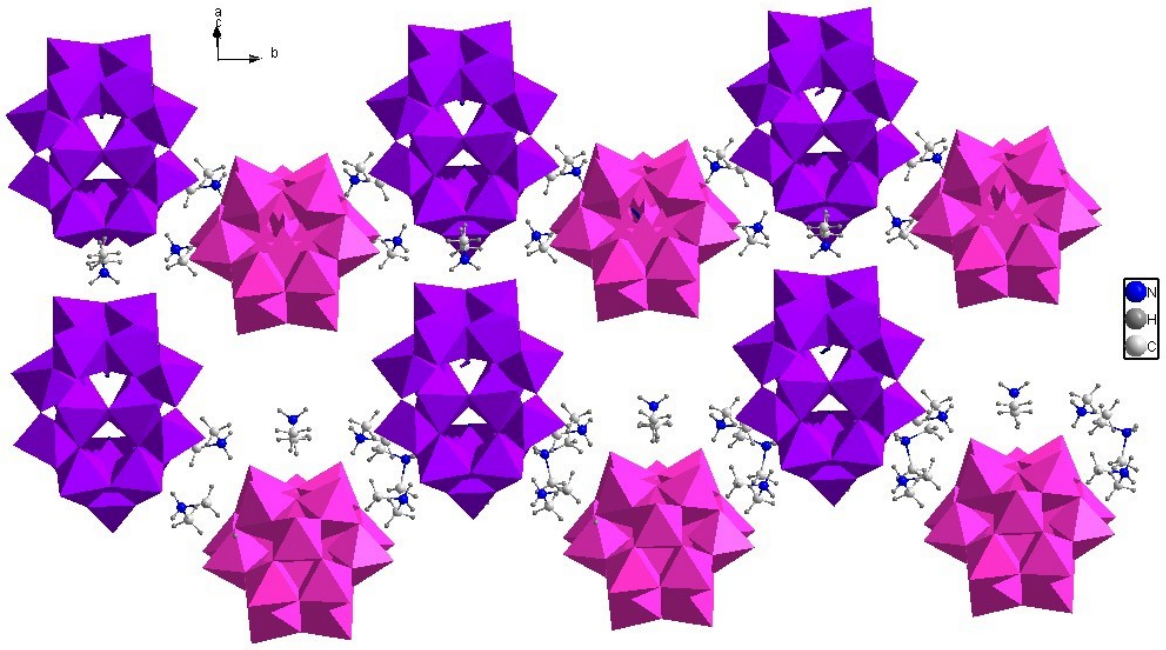

Figure S11: Polyhedral representation showing the $[H_9Cu_2Mo_{18}O_{62}]^{3-}$ anions as alternating purple and pink polyhedra; dimethylamine cations are depicted in ball-and-stick form.

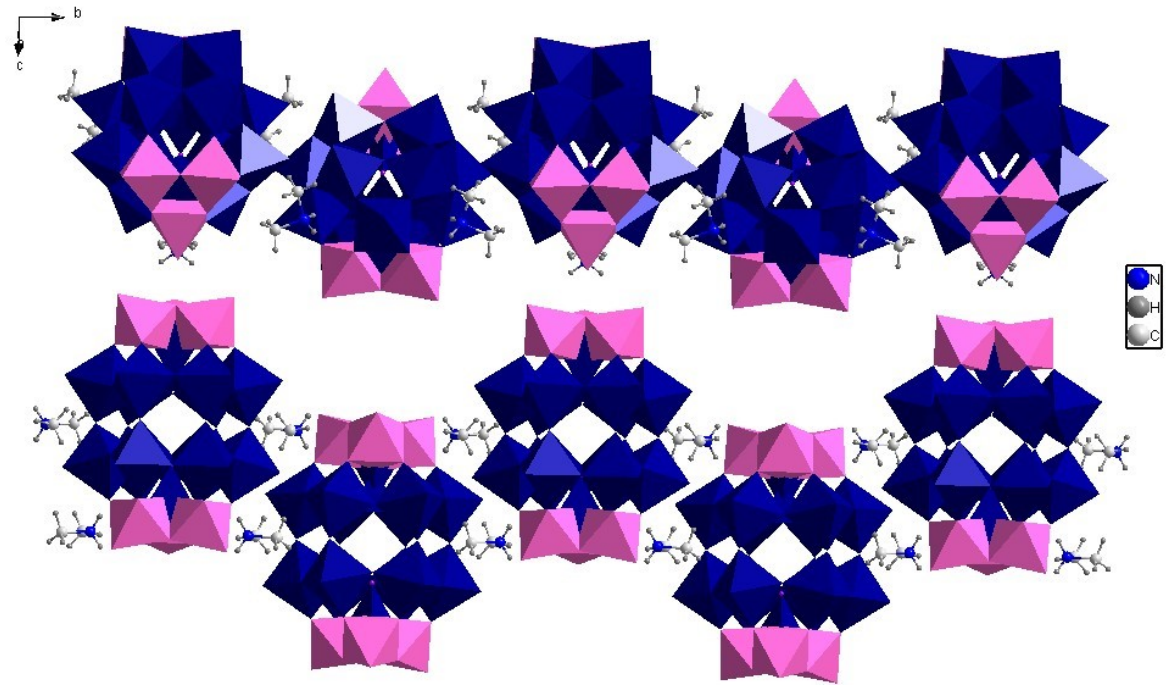

Figure S12: The 1D framework of $[(DMA)]^{3+}$ $[H_9Cu_2Mo_{18}O_{62}]^{3-}$ (**1**) viewed along the *a*-axis. The Dawson-type $[H_9Cu_2Mo_{18}O_{62}]^{3-}$ polyoxometalate units are depicted as interconnected blue belt-shaped and pink cap-shaped polyhedra, emphasizing the structural organization of the anionic cluster. The DMA^+ ions are illustrated in a ball-and-stick representation, highlighting their spatial distribution and stabilization role within the crystal lattice.

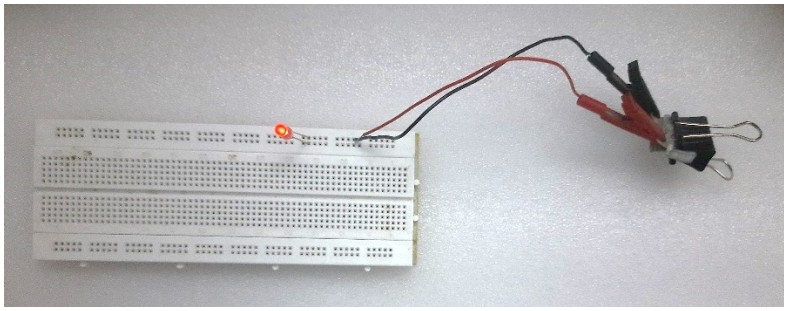

Figure S13. Working prototype of the symmetric supercapacitor device.

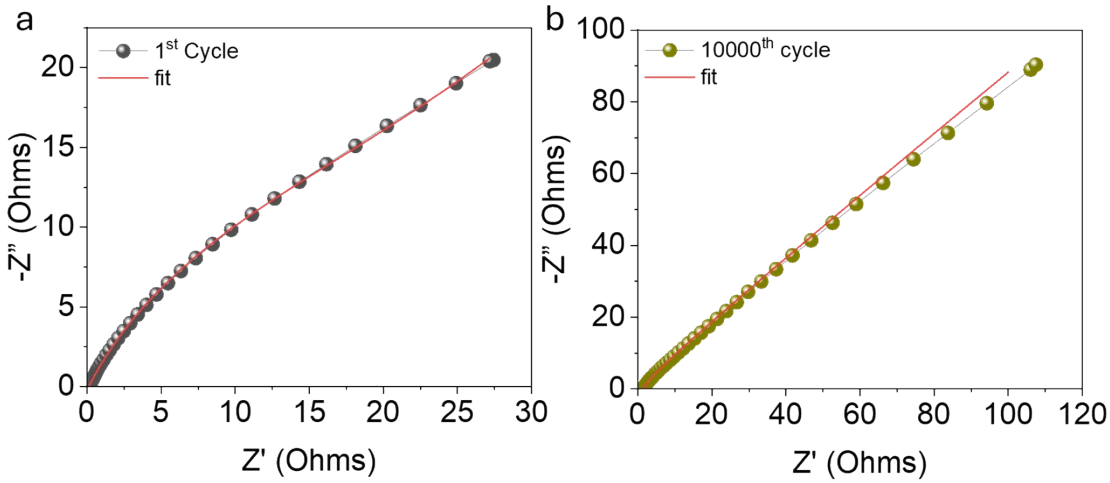

Figure S14. (a) EIS before cycling test (b) EIS after 10000 cycle test.

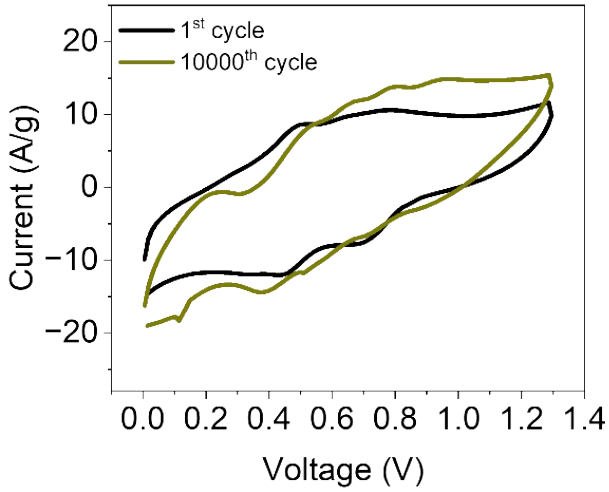

Figure S15: Cyclic Stability test of Sym-SC after 10000 cycles by CV (scan rate 1 V/s).

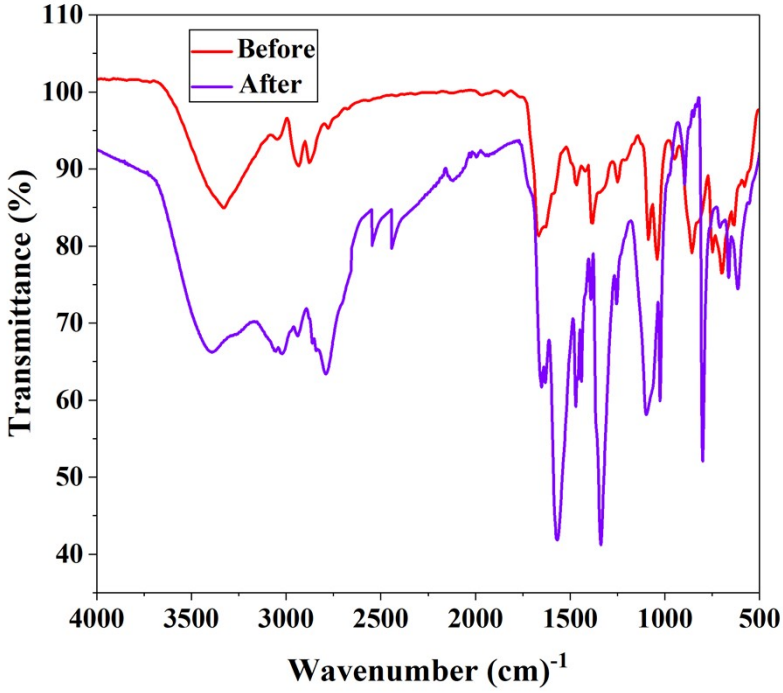

Figure 16: Fourier transform-infra-red (FT-IR) spectrum of recover of **1**.

Table S1. Crystallographic Data and Refinement Parameters of Complex **1.**

Parameter	**1**
Empirical formula	$C_6H_{24}Cu_2Mo_{18}N_3O_{62}$
FW (g mol^{-1})	2984.28
Temperature/K	295.0

Crystal System	Orthorhombic
Space group	Pnma
a (A)	20.9100(16)
b (A)	19.5047(16)
c (A)	23.230(2)
α (◦)	90
β (◦)	90
γ (◦)	90
Volume /(A°3)	9474.1(13)
Z	4
ρ_{calcd} (g cm^{-3})	2.092
μ (mm^{-1})	2.808
F(000)	5564.0
Crystal size/mm3	0.23 × 0.21 × 0.19
Radiation	MoKα (λ = 0.71073
2θ range for data collection/°	3.35 to 48.812
Index ranges	-24 ≤ h ≤ 24, -22 ≤ k ≤ 22, -27 ≤ l ≤ 27
Collected Reflections	55564
Independent reflections	8024 [R_{int} = 0.0788, R_{sigma} = 0.0486]
Parameters	8024/557/436
Goodness-of-fit on F^2	1.035
Final R indexes [I>=2σ (I)]	R_1 = 0.1030, wR_2 = 0.2755
Final R indexes [all data]	R_1 = 0.1324, wR_2 = 0.3117
Largest diff. peak/hole/ e $Å^{-3}$	2.44/-5.53

Table S2. Electrochemical Performance Comparison of State-of-the-Art polyoxomolybdate Electrodes for Supercapacitors.

Entry	Electrode Material	Electrolyte	Specific Capacitance (Fg^{-1})	% Retention	Current density/ Scan rate	Ref
1	$H_3PMo_{12}O_{40}//H_xRuO_2$	Nafion117	$112Fg^{-1}$	-	2.2 $mAcm^{-2}$	9
2	$H_3PMo_{12}O_{40}$/PAni	Poly(2,5-benzimidazole)	195 mF cm^{-2}	2000^{th} (~85 %)	0.125 $mAcm^{-2}$	10
3	$H_3PMo_{12}O_{40}$/PAni	Nafion117	168 Fg^{-1}	200^{th} (~60 %)	$0.4Ag^{-1}$	11
4	$H_3PMo_{12}O_{40}$/PAni	Nafion117+acid	110 Fg^{-1}	4000^{th} (~68 %)	$0.4Ag^{-1}$	12
6	$H_3PMo_{12}O_{40}$/PPy	Nafion115	$22.9Fg^{-1}$	-	$1mVs^{-1}$	13
8	$H_5PV_2Mo_{10}O_{40}$/PPy	Nafion115	$27.6Fg^{-1}$	-	$1mVs^{-1}$	13
10	$H_4SiMo_{12}O_{40}$/PPy	Nafion115	$33.4Fg^{-1}$	-	$1mVs^{-1}$	13
11	$H_3PMo_{12}O_{40}$/PPy//$H_3PW_{12}O_{40}$/PEDOT	0.5M H_2SO_4	$31Fg^{-1}$	200^{th} (~68%)	1mA	14
12	$H_3PMo_{12}O_{40}$/PEDOT	0.1M H_2SO_4	$140Fg^{-1}$	-	$10mVs^{-1}$	15
13	$H_5PV_2Mo_{10}O_{40}$/PEDOT	0.1M H_2SO_4	$70Fg^{-1}$	-	$10mVs^{-1}$	15
14	$Cs_XPMo_{12}O_{40}$/MWCNT	Nafion117+acid	$285Fg^{-1}$	500^{th} (~65 %)	$0.2Ag^{-1}$	16
15	$H_3PMo_{12}O_{40}$/MWCNT	1M H_2SO_4	$38Fg^{-1}$	-	$1Ag^{-1}$	17
16	$H_3PMo_{12}O_{40}$/PDDA/Carbon nanoparticles	1M H_2SO_4	0.6F cm^{-2}	-	$5Vs^{-1}$	18
17	$H_3PMo_{12}O_{40}$/PDDAd/MWCNT	1M H_2SO_4	2.68F cm^{-2}	-	$50mVs^{-1}$	19
18	$H_3PMo_{12}O_{40}$/PDDA/MWCNT	1M H_2SO_4	1.93F cm^{-2}	-	$50mVs^{-1}$	19

21	$H_3PMo_{12}O_{40}$/AC	1M H_2SO_4	140Fg^{-1}	8000th (~91 %)	1Ag^{-1}	[20]
22	SWCNT-TBA-PV_2Mo_{10}	1M H_2SO_4	317mF cm^{-2}	6500 (~95%)	0.1 mA cm^{-2}	[21]
24	PMo_{12} mixed with PW_{12}	1 M H_2SO_4	96 F cm^{-3}	-	-	[22]
25	Mo_{132}-DTAB-EEG	1 M H_2SO_4	65 F g^{-1}, 93 F cm^3, 93 mF cm^2	5000 (~99 %)	1 mV s^{-1}	[23]
26	[Ni(itmb)$_4$($HPMo_{12}O_{40}$)]·2 H_2O	2M H_3PO_4	477.9 F g^{-1}	-	15 A g^{-1}	[24]
27	[Mo_{132}]-rGO	1M Li_2SO_4	617.3 Fg^{-1}	-		[25]
28	**[(DMA)$_3$]$^{3+}$[$H_9Cu_2Mo_{18}O_{62}$]$^{3-}$**	**1 M H_2SO_4**	**197.27 F g^{-1}**	**5000 (82.70 %)**	**5 mV s^{-1}**	**Present work**

List of abbreviations: PAni-Polyaniline, PPy-Polypyrrole, PEDOT-Poly (3,4-Ethylene dioxy thiophene), PDDA-Poly (diallyl dimethyl ammonium) chloride, MWCNT-multiwalled carbon nanotubes, SWNCT- single-walled carbon nanotubes, TBA-tetra n-butyl ammonium, AC-activated carbon, DTAB-dodecyl trimethyl ammonium bromide, EEG-electrochemically exfoliated graphene, itmb-1-(imidazo-1-ly)-4-(1,2,4-triazol-1-ylmethyl) benzene, rGO-reduced graphene oxide.

S7. Experimental interatomic distances (Å), bond angle, torsion angle and dihedral angle of 1:

Table S3: Fractional Atomic Coordinates (×10^4) and Equivalent Isotropic Displacement Parameters (Å^2×10^3) for **1** . U_{eq} is defined as 1/3 of of the trace of the orthogonalised U_{IJ} tensor.

Atom	*x*	*y*	*z*	U(eq)
Mo(6)	1136.7(7)	3445.2(9)	3396.1(7)	36.4(4)
Mo(5)	365.5(8)	3449.9(8)	4852.4(7)	38.8(4)
Mo(8)	3815.5(7)	3391.5(8)	4547.8(7)	35.5(4)
Mo(7)	2428.8(8)	4340.3(8)	3957.2(7)	38.6(4)
Mo(9)	3512.5(8)	3392.3(9)	2974.0(7)	41.5(5)

Mo(10)	2223.5(11)	2500	2408.5(10)	42.6(6)
Mo(3)	3043.5(9)	3391.4(8)	5997.4(7)	40.9(5)
Mo(4)	1656.4(9)	4345.0(8)	5412.5(8)	41.5(5)
Mo(1)	178.1(14)	2500	6227.0(12)	52.1(7)
Mo(2)	1464.9(11)	3388.2(10)	6789.0(8)	54.3(6)
Cu(2)	2467(2)	2500	3942.3(18)	63.3(11)
Cu(1)	1667(2)	2500	5444(2)	69.9(12)
O(25)	3895(6)	3315(7)	3706(6)	44(3)
O(28)	2767(8)	2500	3347(7)	37(3)
O(22)	4189(8)	2500	4609(8)	41(4)
O(17)	293(10)	2500	4703(8)	49(4)
O(15)	783(6)	4231(7)	5151(6)	47(3)
O(34)	2898(7)	3171(8)	2365(5)	53(3)
O(35)	3872(8)	2500	2794(8)	50(4)
O(19)	1933(7)	4371(7)	4651(6)	47(3)
O(37)	743(6)	3578(7)	4117(6)	46(3)
O(3)	188(7)	3177(8)	5660(6)	52(3)
O(33)	1959(12)	2500	1727(10)	99(7)
O(11)	2449(7)	3997(7)	5622(6)	48(3)
O(7)	1385(7)	3990(8)	6178(6)	53(3)
O(32)	1727(6)	1826(8)	2751(6)	51(3)
O(27)	2901(6)	3969(8)	3278(5)	48(3)
O(12)	2350(9)	2500	5539(8)	44(4)
O(29)	1654(6)	4242(7)	3513(6)	43(3)
O(2)	1349(9)	2500	6019(8)	47(4)
O(26)	2575(7)	5167(7)	3862(7)	58(4)
O(24)	3508(7)	3305(7)	5305(6)	48(3)
O(9)	3312(10)	2500	6254(9)	52(4)
O(31)	560(6)	3770(7)	2995(6)	51(3)
O(21)	3131(7)	3999(7)	4381(5)	47(3)
O(8)	2359(8)	3305(7)	6601(6)	54(3)

O(5)	1550(13)	2500	7139(9)	70(5)
O(23)	4438(7)	3911(7)	4669(6)	52(3)
O(30)	977(9)	2500	3457(9)	47(4)
O(13)	1683(8)	5165(7)	5578(7)	62(4)
O(10)	3540(8)	3884(8)	6375(6)	60(4)
O(1)	568(9)	3177(9)	6727(7)	71(4)
O(16)	-361(6)	3782(8)	4700(6)	52(3)
O(36)	3999(7)	3921(9)	2634(7)	70(4)
O(6)	1496(9)	3911(10)	7378(6)	77(5)
O(4)	-567(12)	2500	6444(10)	76(6)
N(2)	-46(14)	5574(12)	3734(12)	100(8)
O(20)	2977(8)	2500	4356(7)	33(3)
O(18)	2094(6)	1900(6)	3987(5)	38(3)
C(3)	609(18)	5390(20)	4045(17)	122(11)
O(14)	1457(7)	3128(7)	5138(6)	46(3)
C(4)	-258(19)	4868(16)	3616(19)	131(13)
N(1)	3725(15)	2500	1493(12)	87(11)
C(1)	4366(18)	2500	1533(15)	99(7)
C(2)	3526(19)	2500	748(15)	99(7)

Table S4: Anisotropic Displacement Parameters ($Å^2 \times 10^3$) for **1**. The Anisotropic displacement factor exponent takes the form: $-2\pi^2[h^2a^{*2}U_{11}+2hka^*b^*U_{12}+\ldots]$.

Atom	$\mathbf{U_{11}}$	$\mathbf{U_{22}}$	$\mathbf{U_{33}}$	$\mathbf{U_{23}}$	$\mathbf{U_{13}}$	$\mathbf{U_{12}}$
Mo(6)	28.5(8)	43.9(10)	36.9(9)	5.6(7)	-0.1(7)	4.8(7)
Mo(5)	34.3(9)	40.5(9)	41.7(9)	1.1(7)	7.3(7)	7.0(7)
Mo(8)	31.4(8)	37.4(9)	37.7(9)	-1.1(7)	-2.1(7)	-4.3(6)
Mo(7)	39.3(9)	32.9(9)	43.7(9)	8.3(7)	3.2(7)	0.3(7)
Mo(9)	32.1(9)	57.8(11)	34.6(9)	5.8(8)	7.6(7)	-5.5(7)

Mo(10)	31.8(12)	67.1(16)	29.0(12)	0	1.6(10)	0
Mo(3)	53.0(11)	35.2(9)	34.3(9)	-6.3(7)	-5.4(8)	-3.1(7)
Mo(4)	51.5(10)	28.2(8)	44.7(10)	-4.4(7)	6.0(8)	1.5(7)
Mo(1)	56.9(16)	51.6(15)	47.7(15)	0	24.9(13)	0
Mo(2)	80.8(15)	47.4(11)	34.8(10)	-8.6(8)	12.2(9)	-1.1(9)
Cu(2)	69(3)	63(3)	57(2)	0	5(2)	0
Cu(1)	87(3)	58(3)	65(3)	0	8(2)	0
O(25)	30(6)	65(8)	38(6)	1(5)	2(5)	-4(5)
O(28)	28(7)	57(9)	27(7)	0	6(6)	0
O(22)	20(7)	45(8)	59(10)	0	-4(7)	0
O(17)	52(11)	50(9)	44(10)	0	-7(9)	0
O(15)	46(6)	47(7)	49(7)	-6(6)	12(5)	-5(5)
O(34)	44(7)	80(9)	34(6)	16(6)	3(5)	7(6)
O(35)	27(8)	80(10)	42(10)	0	3(7)	0
O(19)	65(8)	37(7)	41(6)	3(5)	12(6)	7(6)
O(37)	39(7)	51(7)	48(6)	7(5)	11(5)	10(6)
O(3)	50(7)	59(8)	46(6)	3(6)	14(6)	-4(6)
O(33)	58(9)	200(20)	39(8)	0	2(7)	0
O(11)	59(7)	39(6)	46(7)	-1(6)	7(5)	2(5)
O(7)	54(8)	54(7)	52(7)	-6(6)	7(6)	1(6)
O(32)	21(6)	72(9)	61(8)	-10(7)	5(6)	-3(6)
O(27)	44(7)	65(7)	36(6)	10(6)	8(5)	-1(6)
O(12)	38(8)	43(8)	51(10)	0	3(6)	0

O(29)	36(6)	45(7)	47(7)	1(6)	13(5)	2(5)
O(2)	51(8)	42(9)	47(8)	0	15(7)	0
O(26)	65(9)	49(8)	61(9)	16(6)	5(7)	-7(6)
O(24)	48(7)	49(8)	48(6)	-4(5)	1(5)	-2(5)
O(9)	53(10)	57(10)	45(10)	0	1(8)	0
O(31)	38(7)	57(8)	57(7)	15(7)	-2(6)	12(6)
O(21)	52(6)	51(7)	37(6)	6(6)	0(5)	-4(6)
O(8)	83(8)	50(8)	29(6)	-4(5)	5(6)	7(6)
O(5)	95(15)	75(11)	40(10)	0	11(10)	0
O(23)	57(7)	50(7)	50(8)	-2(6)	-10(6)	-25(7)
O(30)	33(9)	50(9)	58(12)	0	8(9)	0
O(13)	71(10)	39(7)	77(10)	-15(6)	10(8)	0(6)
O(10)	72(9)	71(9)	38(7)	-11(7)	-3(7)	-13(8)
O(1)	86(9)	71(10)	55(8)	-12(7)	21(7)	5(7)
O(16)	36(6)	67(9)	53(8)	-5(7)	10(5)	12(6)
O(36)	52(8)	88(10)	72(10)	32(9)	19(7)	-12(8)
O(6)	101(13)	90(10)	40(7)	-23(8)	25(8)	0(10)
O(4)	74(12)	98(18)	55(14)	0	36(10)	0
N(2)	123(18)	71(13)	107(19)	45(13)	9(15)	-7(13)
O(20)	28(7)	41(8)	30(7)	0	-7(6)	0
O(18)	39(6)	31(6)	44(7)	-5(5)	0(5)	-9(5)
C(3)	120(20)	110(20)	140(30)	30(20)	35(17)	60(17)
O(14)	48(6)	46(7)	45(7)	0(5)	8(5)	-1(5)

C(4)	130(20)	70(15)	200(40)	-10(20)	80(20)	20(15)
N(1)	59(11)	150(30)	50(11)	0	-8(11)	0
C(1)	58(9)	200(20)	39(8)	0	2(7)	0
C(2)	58(9)	200(20)	39(8)	0	2(7)	0

Table S5: Bond Lengths for **1.**

Atom	**Atom**	**Length/Å**	**Atom**	**Atom**	**Length/Å**
Mo(6)	O(37)	1.883(13)	Mo(3)	O(11)	1.924(14)
Mo(6)	O(32)[1]	2.012(14)	Mo(3)	O(12)	2.503(14)
Mo(6)	O(29)	1.913(13)	Mo(3)	O(24)	1.886(14)
Mo(6)	O(31)	1.651(13)	Mo(3)	O(9)	1.922(9)
Mo(6)	O(30)	1.879(4)	Mo(3)	O(8)	2.010(15)
Mo(6)	O(18)[1]	2.519(12)	Mo(3)	O(10)	1.665(15)
Mo(5)	O(17)	1.891(4)	Mo(4)	O(15)	1.937(14)
Mo(5)	O(15)	1.887(14)	Mo(4)	O(19)	1.862(13)
Mo(5)	O(37)	1.899(13)	Mo(4)	O(11)	1.856(14)
Mo(5)	O(3)	1.985(14)	Mo(4)	O(7)	1.992(15)
Mo(5)	O(16)	1.690(13)	Mo(4)	O(13)	1.647(14)
Mo(5)	O(14)	2.458(14)	Mo(4)	O(14)	2.493(14)
Mo(8)	O(25)	1.969(13)	Mo(1)	O(3)[1]	1.866(14)
Mo(8)	O(22)	1.911(7)	Mo(1)	O(3)	1.866(14)
Mo(8)	O(24)	1.880(14)	Mo(1)	O(2)	2.49(2)

Mo(8)	O(21)	1.897(14)	Mo(1)	O(1)[1]	1.938(18)
Mo(8)	O(23)	1.673(13)	Mo(1)	O(1)	1.938(18)
Mo(8)	O(20)	2.510(11)	Mo(1)	O(4)	1.64(2)
Mo(7)	O(19)	1.917(13)	Mo(2)	O(7)	1.848(15)
Mo(7)	O(27)	1.997(13)	Mo(2)	O(2)	2.502(14)
Mo(7)	O(29)	1.931(14)	Mo(2)	O(8)	1.926(17)
Mo(7)	O(26)	1.656(14)	Mo(2)	O(5)	1.922(10)
Mo(7)	O(21)	1.889(14)	Mo(2)	O(1)	1.926(19)
Mo(7)	O(18)[1]	2.519(12)	Mo(2)	O(6)	1.708(15)
Mo(9)	O(25)	1.885(13)	Cu(2)	O(28)	1.519(16)
Mo(9)	O(28)	2.492(12)	Cu(2)	O(20)	1.434(16)
Mo(9)	O(34)	1.959(14)	Cu(2)	O(18)	1.411(12)
Mo(9)	O(35)	1.942(8)	Cu(2)	O(18)[1]	1.411(12)
Mo(9)	O(27)	1.843(14)	Cu(1)	O(12)	1.444(19)
Mo(9)	O(36)	1.650(14)	Cu(1)	O(2)	1.493(19)
Mo(10)	O(28)	2.458(17)	Cu(1)	O(14)[1]	1.482(14)
Mo(10)	O(34)[1]	1.928(15)	Cu(1)	O(14)	1.482(14)
Mo(10)	O(34)	1.928(15)	N(2)	C(3)	1.59(4)
Mo(10)	O(33)	1.68(2)	N(2)	C(4)	1.47(4)
Mo(10)	O(32)[1]	1.854(14)	N(1)	C(1)	1.34(5)
Mo(10)	O(32)	1.854(14)	N(1)	C(2)	1.78(4)

[1]+X,1/2-Y,+Z

Table S6: Bond Angles for **1**.

Atom	Atom	Atom	Angle/°	Atom	Atom	Atom	Angle/°
O(37)	Mo(6)	O(32)[1]	165.0(6)	O(15)	Mo(4)	O(7)	88.4(6)
O(37)	Mo(6)	O(29)	90.5(6)	O(15)	Mo(4)	O(14)	69.7(5)
O(37)	Mo(6)	O(18)[1]	84.2(5)	O(19)	Mo(4)	O(15)	89.9(6)
O(32)[1]	Mo(6)	O(18)[1]	81.3(5)	O(19)	Mo(4)	O(7)	161.2(6)
O(29)	Mo(6)	O(32)[1]	88.4(6)	O(19)	Mo(4)	O(14)	80.5(5)
O(29)	Mo(6)	O(18)[1]	72.0(5)	O(11)	Mo(4)	O(15)	151.8(6)
O(31)	Mo(6)	O(37)	97.5(6)	O(11)	Mo(4)	O(19)	88.9(6)
O(31)	Mo(6)	O(32)[1]	97.4(6)	O(11)	Mo(4)	O(7)	83.9(6)
O(31)	Mo(6)	O(29)	100.4(7)	O(11)	Mo(4)	O(14)	82.4(5)
O(31)	Mo(6)	O(30)	106.8(8)	O(7)	Mo(4)	O(14)	81.3(5)
O(31)	Mo(6)	O(18)[1]	172.3(6)	O(13)	Mo(4)	O(15)	102.6(7)
O(30)	Mo(6)	O(37)	89.5(7)	O(13)	Mo(4)	O(19)	100.7(7)
O(30)	Mo(6)	O(32)[1]	84.7(7)	O(13)	Mo(4)	O(11)	105.3(7)
O(30)	Mo(6)	O(29)	152.5(7)	O(13)	Mo(4)	O(7)	98.0(7)
O(30)	Mo(6)	O(18)[1]	80.7(7)	O(13)	Mo(4)	O(14)	172.2(7)
O(17)	Mo(5)	O(37)	89.9(7)	O(3)	Mo(1)	O(3)[1]	90.2(9)
O(17)	Mo(5)	O(3)	84.0(7)	O(3)	Mo(1)	O(2)	81.5(5)
O(17)	Mo(5)	O(14)	82.7(7)	O(3)[1]	Mo(1)	O(2)	81.5(5)
O(15)	Mo(5)	O(17)	153.5(7)	O(3)[1]	Mo(1)	O(1)	154.3(7)
O(15)	Mo(5)	O(37)	91.8(6)	O(3)[1]	Mo(1)	O(1)[1]	86.3(7)
O(15)	Mo(5)	O(3)	87.5(6)	O(3)	Mo(1)	O(1)[1]	154.3(7)
O(15)	Mo(5)	O(14)	71.2(5)	O(3)	Mo(1)	O(1)	86.3(7)

O(37)	Mo(5)	O(3)	164.5(6)	O(1)[1]	Mo(1)	O(2)	72.7(6)
O(37)	Mo(5)	O(14)	83.7(5)	O(1)	Mo(1)	O(2)	72.7(6)
O(3)	Mo(5)	O(14)	81.3(5)	O(1)[1]	Mo(1)	O(1)	85.8(11)
O(16)	Mo(5)	O(17)	105.4(8)	O(4)	Mo(1)	O(3)	103.2(8)
O(16)	Mo(5)	O(15)	100.6(7)	O(4)	Mo(1)	O(3)[1]	103.2(8)
O(16)	Mo(5)	O(37)	97.8(6)	O(4)	Mo(1)	O(2)	173.2(10)
O(16)	Mo(5)	O(3)	97.6(6)	O(4)	Mo(1)	O(1)[1]	102.5(8)
O(16)	Mo(5)	O(14)	171.7(6)	O(4)	Mo(1)	O(1)	102.5(8)
O(25)	Mo(8)	O(20)	80.2(5)	O(7)	Mo(2)	O(2)	83.2(6)
O(22)	Mo(8)	O(25)	88.3(7)	O(7)	Mo(2)	O(8)	88.1(6)
O(22)	Mo(8)	O(20)	70.6(5)	O(7)	Mo(2)	O(5)	154.9(7)
O(24)	Mo(8)	O(25)	162.1(6)	O(7)	Mo(2)	O(1)	89.5(7)
O(24)	Mo(8)	O(22)	89.4(7)	O(8)	Mo(2)	O(2)	82.7(6)
O(24)	Mo(8)	O(21)	89.4(6)	O(5)	Mo(2)	O(2)	71.8(7)
O(24)	Mo(8)	O(20)	82.2(6)	O(5)	Mo(2)	O(8)	86.0(9)
O(21)	Mo(8)	O(25)	84.7(6)	O(5)	Mo(2)	O(1)	85.9(10)
O(21)	Mo(8)	O(22)	153.0(6)	O(1)	Mo(2)	O(2)	72.8(6)
O(21)	Mo(8)	O(20)	82.5(5)	O(1)	Mo(2)	O(8)	155.5(6)
O(23)	Mo(8)	O(25)	98.4(6)	O(6)	Mo(2)	O(7)	103.9(8)
O(23)	Mo(8)	O(22)	102.8(7)	O(6)	Mo(2)	O(2)	171.8(7)
O(23)	Mo(8)	O(24)	99.4(7)	O(6)	Mo(2)	O(8)	101.3(8)
O(23)	Mo(8)	O(21)	104.0(7)	O(6)	Mo(2)	O(5)	101.2(9)
O(23)	Mo(8)	O(20)	173.2(6)	O(6)	Mo(2)	O(1)	103.0(8)

O(19)	Mo(7)	O(27)	160.5(6)	O(20)	Cu(2)	O(28)	107.6(10)
O(19)	Mo(7)	O(29)	90.0(6)	O(18)[1]	Cu(2)	O(28)	107.2(6)
O(19)	Mo(7)	O(18)[1]	81.7(5)	O(18)	Cu(2)	O(28)	107.2(6)
O(27)	Mo(7)	O(18)[1]	79.1(5)	O(18)	Cu(2)	O(20)	111.2(6)
O(29)	Mo(7)	O(27)	87.5(5)	O(18)[1]	Cu(2)	O(20)	111.2(6)
O(29)	Mo(7)	O(18)[1]	71.7(5)	O(18)[1]	Cu(2)	O(18)	112.1(11)
O(26)	Mo(7)	O(19)	100.5(7)	O(12)	Cu(1)	O(2)	107.7(11)
O(26)	Mo(7)	O(27)	99.0(7)	O(12)	Cu(1)	O(14)[1]	111.5(7)
O(26)	Mo(7)	O(29)	100.4(7)	O(12)	Cu(1)	O(14)	111.5(7)
O(26)	Mo(7)	O(21)	105.6(7)	O(14)	Cu(1)	O(2)	107.2(7)
O(26)	Mo(7)	O(18)[1]	171.9(6)	O(14)[1]	Cu(1)	O(2)	107.2(7)
O(21)	Mo(7)	O(19)	89.6(6)	O(14)[1]	Cu(1)	O(14)	111.5(11)
O(21)	Mo(7)	O(27)	84.2(6)	Mo(9)	O(25)	Mo(8)	148.6(7)
O(21)	Mo(7)	O(29)	153.6(6)	Mo(9)[1]	O(28)	Mo(9)	88.6(5)
O(21)	Mo(7)	O(18)[1]	82.1(5)	Mo(10)	O(28)	Mo(9)[1]	88.9(5)
O(25)	Mo(9)	O(28)	84.1(6)	Mo(10)	O(28)	Mo(9)	88.9(5)
O(25)	Mo(9)	O(34)	155.8(6)	Cu(2)	O(28)	Mo(9)[1]	125.1(6)
O(25)	Mo(9)	O(35)	87.6(7)	Cu(2)	O(28)	Mo(9)	125.1(6)
O(34)	Mo(9)	O(28)	71.8(6)	Cu(2)	O(28)	Mo(10)	128.1(9)
O(35)	Mo(9)	O(28)	72.0(5)	Mo(8)	O(22)	Mo(8)[1]	130.9(9)
O(35)	Mo(9)	O(34)	84.3(7)	Mo(5)[1]	O(17)	Mo(5)	157.0(11)
O(27)	Mo(9)	O(25)	89.9(6)	Mo(5)	O(15)	Mo(4)	130.1(8)
O(27)	Mo(9)	O(28)	81.9(5)	Mo(10)	O(34)	Mo(9)	126.3(7)

O(27)	Mo(9)	O(34)	87.5(6)	Mo(9)	O(35)	Mo(9)[1]	127.4(9)
O(27)	Mo(9)	O(35)	153.9(6)	Mo(4)	O(19)	Mo(7)	165.0(9)
O(36)	Mo(9)	O(25)	102.7(7)	Mo(6)	O(37)	Mo(5)	164.5(8)
O(36)	Mo(9)	O(28)	171.3(7)	Mo(1)	O(3)	Mo(5)	149.2(9)
O(36)	Mo(9)	O(34)	101.2(7)	Mo(4)	O(11)	Mo(3)	157.0(8)
O(36)	Mo(9)	O(35)	102.6(8)	Mo(2)	O(7)	Mo(4)	151.7(8)
O(36)	Mo(9)	O(27)	103.3(8)	Mo(10)	O(32)	Mo(6)[1]	148.1(8)
O(34)	Mo(10)	O(28)	73.0(5)	Mo(9)	O(27)	Mo(7)	150.1(8)
O(34)[1]	Mo(10)	O(28)	73.0(5)	Mo(3)	O(12)	Mo(3)[1]	88.0(6)
O(34)	Mo(10)	O(34)[1]	85.6(9)	Cu(1)	O(12)	Mo(3)	129.6(5)
O(33)	Mo(10)	O(28)	171.7(10)	Cu(1)	O(12)	Mo(3)[1]	129.6(5)
O(33)	Mo(10)	O(34)[1]	101.1(7)	Mo(6)	O(29)	Mo(7)	129.1(7)
O(33)	Mo(10)	O(34)	101.1(7)	Mo(1)	O(2)	Mo(2)	87.5(5)
O(33)	Mo(10)	O(32)	102.7(8)	Mo(1)	O(2)	Mo(2)[1]	87.5(5)
O(33)	Mo(10)	O(32)[1]	102.7(7)	Mo(2)[1]	O(2)	Mo(2)	87.7(6)
O(32)	Mo(10)	O(28)	83.0(5)	Cu(1)	O(2)	Mo(1)	127.6(12)
O(32)[1]	Mo(10)	O(28)	83.0(5)	Cu(1)	O(2)	Mo(2)[1]	126.6(6)
O(32)	Mo(10)	O(34)[1]	87.2(6)	Cu(1)	O(2)	Mo(2)	126.6(6)
O(32)	Mo(10)	O(34)	156.0(6)	Mo(8)	O(24)	Mo(3)	164.9(9)
O(32)[1]	Mo(10)	O(34)	87.2(6)	Mo(3)	O(9)	Mo(3)[1]	129.5(11)
O(32)[1]	Mo(10)	O(34)[1]	156.0(6)	Mo(7)	O(21)	Mo(8)	155.9(8)
O(32)	Mo(10)	O(32)[1]	90.3(9)	Mo(2)	O(8)	Mo(3)	147.4(8)
O(11)	Mo(3)	O(12)	81.9(5)	Mo(2)[1]	O(5)	Mo(2)	128.6(12)

O(11)	Mo(3)	O(8)	84.7(6)	Mo(6)	O(30)	Mo(6)[1]	157.8(11)
O(24)	Mo(3)	O(11)	90.0(6)	Mo(2)	O(1)	Mo(1)	126.9(8)
O(24)	Mo(3)	O(12)	82.7(6)	C(4)	N(2)	C(3)	97(3)
O(24)	Mo(3)	O(9)	91.9(7)	Mo(8)[1]	O(20)	Mo(8)	87.7(5)
O(24)	Mo(3)	O(8)	162.4(6)	Cu(2)	O(20)	Mo(8)	129.7(5)
O(9)	Mo(3)	O(11)	152.2(7)	Cu(2)	O(20)	Mo(8)[1]	129.7(5)
O(9)	Mo(3)	O(12)	70.9(6)	Mo(6)[1]	O(18)	Mo(7)[1]	87.1(4)
O(9)	Mo(3)	O(8)	85.2(7)	Cu(2)	O(18)	Mo(6)[1]	128.4(8)
O(8)	Mo(3)	O(12)	80.0(6)	Cu(2)	O(18)	Mo(7)[1]	129.9(8)
O(10)	Mo(3)	O(11)	106.7(7)	Mo(5)	O(14)	Mo(4)	88.9(5)
O(10)	Mo(3)	O(12)	170.8(7)	Cu(1)	O(14)	Mo(5)	128.0(8)
O(10)	Mo(3)	O(24)	100.4(7)	Cu(1)	O(14)	Mo(4)	128.0(8)
O(10)	Mo(3)	O(9)	100.2(8)	C(1)	N(1)	C(2)	107(3)
O(10)	Mo(3)	O(8)	97.2(7)				

[1]+X,1/2-Y,+Z

Table S7: Hydrogen Atom Coordinates (Å×10^4) and Isotropic Displacement Parameters (Å^2×10^3) for **1**.

Atom	***X***	***Y***	***z***	**U(eq)**
H(2A)	-314.31	5796.47	3966.29	120
H(2B)	13.99	5815.18	3413.26	120
H(3A)	883.68	5152.34	3778.41	184
H(3B)	523.84	5094.02	4368.42	184

H(3C)	813.44	5798.56	4174.68	184
H(4A)	-346.63	4818.86	3212.18	196
H(4B)	-638.09	4771.41	3832.68	196
H(4C)	73.23	4552.48	3724.6	196
H(1A)	3564.32	2870.33	1663.48	104
H(1B)	3564.32	2129.67	1663.48	104
H(1C)	4489.03	2472.53	1930.09	149
H(1D)	4532.27	2914.9	1367.99	149
H(1E)	4535.34	2112.57	1328.14	149
H(2C)	3910.73	2528.95	523.5	149
H(2D)	3257.88	2886.61	664.59	149
H(2E)	3303.36	2084.44	654.76	149

Table S8: Atomic Occupancy for **1**.

Atom	***Occupancy***	**Atom**	***Occupancy***	**Atom**	***Occupancy***
H(1A)	0.5	H(1B)	0.5	H(1C)	0.5
H(1D)	0.5	H(1E)	0.5	H(2C)	0.5
H(2D)	0.5	H(2E)	0.5		

Table S9: Solvent masks information for **1.**

Number	**X**	**Y**	**Z**	**Volume**	**Electron count**	**Content**
1	-0.935	-0.585	-0.619	4377.0	1496.3	?

References

1. O. V. Dolomanov, L. J. Bourhis, R. J. Gildea, J. A. Howard and H. Puschmann, Applied Crystallography, 2009, **42**, 339-341.
2. G. M. Sheldrick, Acta crystallographica. Section A, Foundations and advances, 2015, **71**, 3-8.
3. G. M. J. F. o. C. Sheldrick, 2015, **71**, 3-8.
4. Y. Kashyap, P. R, R. R. Pandey, A. Andola, D. H. Nagaraju and R. K. Pandey, Journal of Solid State Electrochemistry, 2024, **28**, 3357-3365.
5. L. Xu, Y. Liu, Z. Ding, X. Xu, X. Liu, Z. Gong, J. Li, T. Lu and L. Pan, Small, 2024, **20**, 2307843.
6. A. Andola, R. R. Pandey, Y. Kashyap, H. Pandey, H. Nakanishi and R. K. Pandey, ACS Applied Nano Materials, 2024, **7**, 1701-1712.
7. R. R. Pandey, Y. Kashyap, A. Andola, H. Nakanishi and R. K. Pandey, ChemistrySelect, 2023, **8**, e202302042.
8. R. R. Pandey, A. Andola, H. Pandey and R. K. Pandey, Carbon Letters, 2025, DOI: 10.1007/s42823-025-00909-3.
9. A. Yamada and J. B. Goodenough, Journal of The Electrochemical Society, 1998, **145**, 737.
10. P. Gómez-Romero, M. Chojak, K. Cuentas-Gallegos, J. A. Asensio, P. J. Kulesza, N. Casañ-Pastor and M. Lira-Cantú, Electrochemistry Communications, 2003, **5**, 149-153.
11. J. Vaillant, M. Lira-Cantu, K. Cuentas-Gallegos, N. Casañ-Pastor and P. Gómez-Romero, Progress in Solid State Chemistry, 2006, **34**, 147-159.
12. A. K. Cuentas-Gallegos, M. Lira-Cantú, N. Casañ-Pastor and P. Gómez-Romero, Advanced Functional Materials, 2005, **15**, 1125-1133.
13. A. M. White and R. C. T. Slade, Synthetic Metals, 2003, **139**, 123-131.
14. G. M. Suppes, C. G. Cameron and M. S. Freund, Journal of The Electrochemical Society, 2010, **157**, A1030.
15. A. M. White and R. C. T. Slade, Electrochimica Acta, 2004, **49**, 861-865.
16. A. K. Cuentas-Gallegos, R. Martínez-Rosales, M. Baibarac, P. Gómez-Romero and M. E. Rincón, Electrochemistry Communications, 2007, **9**, 2088-2092.
17. M. Skunik, M. Chojak, I. A. Rutkowska and P. J. Kulesza, Electrochimica Acta, 2008, **53**, 3862-3869.
18. S. Park, K. Lian and Y. Gogotsi, Journal of The Electrochemical Society, 2009, **156**, A921.

19. T. Akter, K. Hu and K. Lian, Electrochimica Acta, 2011, **56**, 4966-4971.
20. V. Ruiz, J. Suárez-Guevara and P. Gomez-Romero, Electrochemistry Communications, 2012, **24**, 35-38.
21. H.-Y. Chen, R. Al-Oweini, J. Friedl, C. Y. Lee, L. Li, U. Kortz, U. Stimming and M. Srinivasan, Nanoscale, 2015, **7**, 7934-7941.
22. M. Genovese, Y. W. Foong and K. Lian, Electrochimica Acta, 2016, **199**, 261-269.
23. D. Pakulski, A. Gorczyński, W. Czepa, Z. Liu, L. Ortolani, V. Morandi, V. Patroniak, A. Ciesielski and P. Samorì, Energy Storage Materials, 2019, **17**, 186-193.
24. G. Wang, T. Chen, C. J. Gómez-García, F. Zhang, M. Zhang, H. Ma, H. Pang, X. Wang and L. Tan, Small, 2020, **16**, 2001626.
25. Y. Dong, L. Chen, W. Chen, X. Zheng, X. Wang and E. Wang, Chemistry – An Asian Journal, 2018, **13**, 3304-3313.